ISSN 1392 - 1207. MECHANIKA. 2010. Nr.5(85)

Shape optimization of a lightweight tetrapod-like superelement

O. Verners*, M. Dobelis**
**Riga Technical University, 16/20 Azenes St, LV-1048, Riga, Latvia, E-mail: Osvalds.Verners@rtu.lv*
***Riga Technical University, 16/20 Azenes St, LV-1048, Riga, Latvia, E-mail: Modris.Dobelis@rtu.lv*

1. Introduction

According to previous findings [1], spatial diamond-type lattices can be considered optimal from maximum stiffness structure points of view. Due to this, the intended application of the lattice is civil and space structures [2]. Considering multiscale application possibilities, another potential application field could be sandwich structures [3, 4].

For mechanical design purposes, a tetrapod-shaped superelement had been partitioned off the lattice structures [5]. Determination of an optimal shape for the superelement according to composite minimum mass – maximum stiffness criteria was the aim of the earlier study [6]. However, the obtained results corresponded to maximum stiffness optimal structures, constrained by upper mass limit. Since these results were not satisfactory from a minimum mass structure viewpoint and could not be considered as a lattice-type geometry, which was assumed to correspond to a lightweight structure, a new study was performed. The optimization task was subsequently redefined as mass minimization under the constraint of maximum allowable displacement.

The parametric shape optimization [7] in combination with topology optimization was again utilized for the task, allowing for the use of the same parameterized geometric model [8], which consequently facilitated comparison with the earlier results. For completeness, the parameterization and optimization schemes, supplemented with new conditions, will be recapitulated.

All the mechanical and optimization calculations for the study were carried out using ANSYS FEM software package (version 11.0). The sampling of experimental points was carried out using optimization software EDA-Opt.

2. Problem settings

2.1. Assumptions

For simplification, it was assumed that the model could be optimized in the range of linear stress-strain relations, allowing the use of Hookean material law, and small deformations. For the study an isotropic lightweight material, corresponding to the properties of amorphous semi-transparent polyethylene terephthalate (density 1370 kg/m^3, Young's modulus 2800 - 3100 MPa), was chosen to model the structure.

Due to lightweight considerations, the superelement was modelled as a shell structure, based on a simplified geometric model (Fig. 1) [8], which was determined by a set of five independent shape parameters defining the superelement's midsurface geometry. For each of the parameters there were lower and upper geometric limits set. The shell thickness *tk* was chosen to be defined as a constant for the initial calculation with the estimate that a thickness distribution function, based on the initial results, in a parametric form *tk*(*x*1, *x*2) (Figs. 2 - 4), would be defined subsequently.

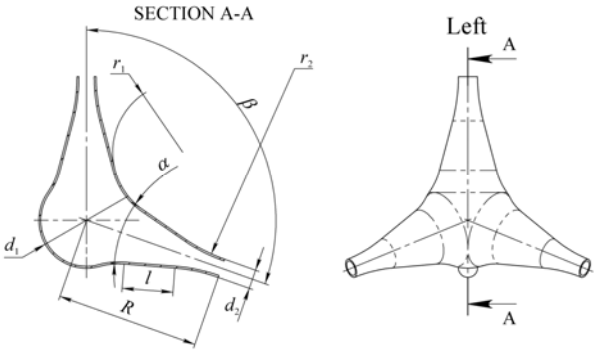

Fig. 1 Parameterized model of a tetrapod-shaped superelement

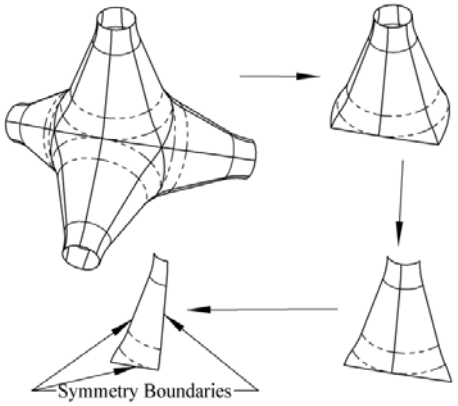

Fig. 2 Derivation of superelement's finite symmetric element

2.2. Input parameters

For the sake of scale-independent superelement's geometric model definition, the values for each of independent linear shape parameter limit were defined with respect to the superelement's ray length *R*, which can be considered as a scaling factor. A size of 75 mm was assumed for the ray length *R*. The rest of independent shape parameters were consequently constrained as

$$tk_{max} < d_2 < \left(tan\left(\beta/2\right)R - tk_{max}/2\right)2 \quad (1)$$

$$tk_{max}/2 < r_{1,2} < R \quad (2)$$

$$0 < \alpha < 90° - \beta/2 \quad (3)$$

$$0 < tk \le tk_{max};\ tk_{max} = k\,R \quad (4)$$

where *k* is coefficient for shell-type geometry.

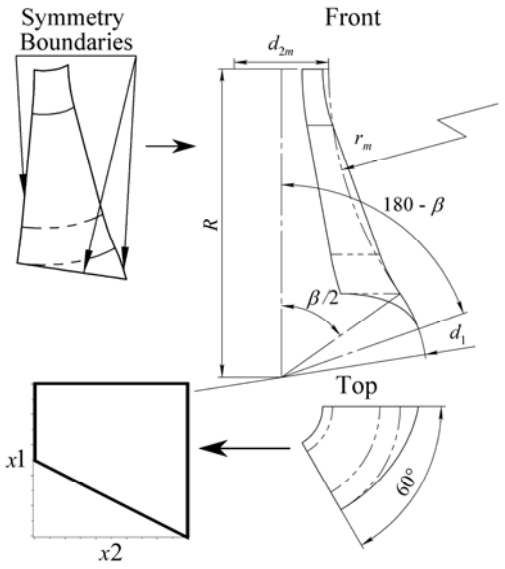

Fig. 3 Descriptive parameterization scheme for superelement's thickness distribution function definition $tk(x1, x2)$, where d_{2m} and r_m are replacement dimensions for d_2 and r_1, r_2, respectively, due to additional approximation

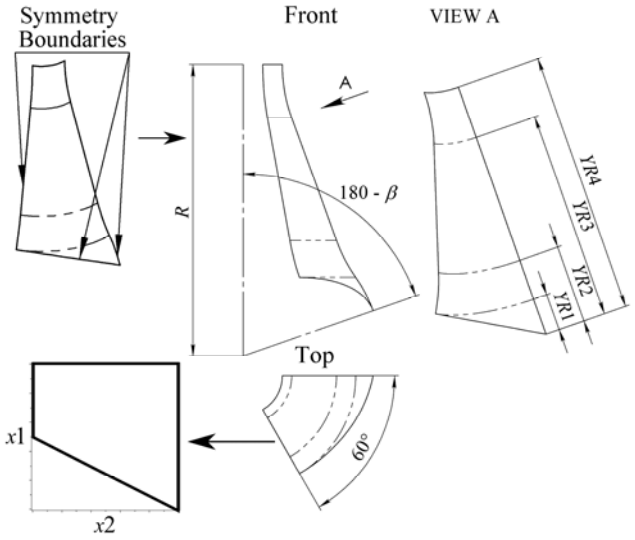

Fig. 4 Descriptive parameterization scheme for superelement's cut definition function $tk(x1, x2)$, where $YR1$-$YR4$ are possible variants for normalizing reference dimensions

2.3. Boundary conditions

Assuming approximate boundary conditions, which would allow the use of symmetries [9] and thereby reduce the computing time, it was possible to partition off a quadrangle-shaped area (Fig. 2) as the finite symmetric element, which corresponds to 1/24 of the superelement and is defined by symmetry planes and a 1/6 portion of the loaded outer edge of a ray. The magnitude of the axially compressive force F (25 N), which corresponds to symmetric loading case (Fig. 5), was chosen with the estimate that the superelement's deadweight effect should be at least an order lower than the axial force and thus could be excluded from the study as negligible. This implied an upper mass limit of 250 g or volume limit of 1.82E+05 mm^3.

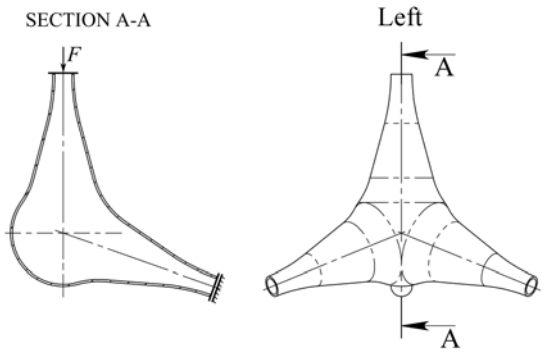

Fig. 5 Superelement's loading scheme, where F is axial loading force

2.4. Output parameters

The output parameters chosen for defining the optimality criteria of superelement's structural optimization include total volume V ($m = V/\rho$, where ρ is material density) and the total strain energy U, which according to [10] is a characteristic for the global stiffness of structures under elastic loading.

An equivalent parameter to strain energy U for the particular loading case could be the displacement u of superelement ray's outer edge under the axial load F, which corresponds to the superelement's axial stiffness, defined as F/u, and also to the work of external forces. For simplicity, the displacement u was expressed with respect to the geometric centre of the superelement. For the displacement u an upper limit of 1.33E-04 R was defined, based on the assumption that a lattice-type geometry should yield deformations larger than those corresponding to a maximum stiffness structure. The particular displacement limit value was derived from the results corresponding to maximum stiffness optimal structure [6], under the mass constraint given above, by defining it as an order greater than the displacement values obtained for the respective structures.

3. Solution scheme

3.1. Parameter correlations

In order to justify the assumptions stated in section 2.4, a further task was a preliminary study of correlations between selected geometric parameters – diameters d_1 and d_2, which represent the overall shape of the superelement – and the chosen output parameters. For calculation of the correlation coefficient values it was chosen to utilize the so-called space-filling experimental designs of Latin hypercube type. The experimental designs can be generated according to various criteria. For the particular task experimental designs were generated according to the Minimal Mean Squared Distance (MMSD) criterion [11]. The correlations between the structural and geometric parameters (Table 1) were evaluated according to the values of Pearson's product-moment correlation coefficient.

A general observation concerns the correlation between mass m and outer edge displacement u, which has a negative value and is significant (-0.5). This confirms the assumption that to different displacement limits different mass ranges and, consequently, different optimal geometries should correspond in accordance with Pareto optima-

lity [7]. The high correlation between the diameters d_1 and d_2 (0.98) allows to conclude that the parameters may be considered equivalent for the correlation study.

Table 1
Correlation coefficient values of superelement's structural response and geometric parameters for constant thickness distribution function (significance level $p < 0.00025$)

	Parameters		
Parameters	d_1	d_2	m
d_1			
d_2	0.98		
m	0.38	0.37	
u	-0.21	-0.20	-0.52

Regarding the correlation between overall superelement's shape, characterized by d_1 or d_2, and structural parameters m and u it should be referred to the respective distributions (Fig. 6) of the 321 space-filling design points which were used for the correlation calculations. It shows that almost linear parallel lines along distribution boundaries, corresponding to minimum or maximum values of m and u for different values of d_1 or d_2, could be drawn. This, in line with the respective correlation values, which are negative for u and positive for m, allows the conclusion that the overall optimal shapes of the superelement should range from bulky or foam-ike, corresponding to large masses and small displacements (also result of the earlier study [6]), to slim or truss-like, which would correspond to larger displacements and small masses (goal of the present study) (Fig. 7).

3.2. Parametric optimization

Since the initial limits of shape parameters included most of the geometrically feasible combinations (see section 2.2), the metamodeling approach [11], also termed subproblem approximation [12], was chosen as the main optimization method. The method is generally classifiable as a zero-order method, since it requires only the values of the dependent variables (objective function and state variables) and not their derivatives. A particular implementation of the method is available as a module of the ANSYS software package (version 11.0), which was used for the study.

A specific task for the implementation of the subproblem method is the definition of design variable sets, required for the definition of approximation functions. The option available within the optimization module of ANSYS is quasirandom sequences. However, since no uniformity of the parameter space was being granted by this method [11], it was chosen to apply the Latin hypercube type experimental design points generated by the optimization software tool EDAOpt [13] according to the MMSD criterion.

The subproblem approximation method can be applied repeatedly after reducing the parameter limits according to the results obtained, thereby obtaining a refined result.

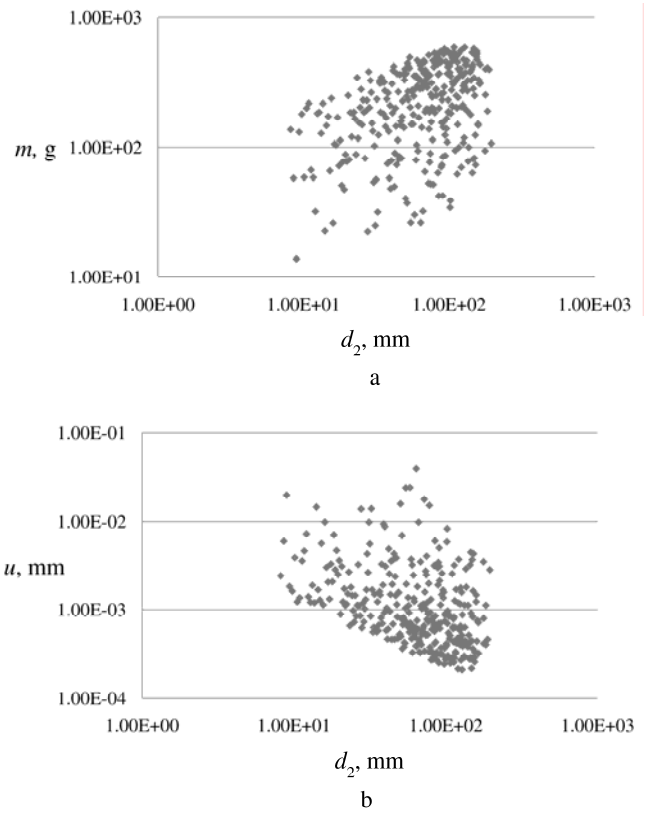

Fig. 6 Distribution of 321 space-filling geometrically consistent design points in the space of total mass m - diameter d_2 (a) and superelement ray's outer edge displacement u - diameter d_2 (b), obtained with constant thickness distribution function

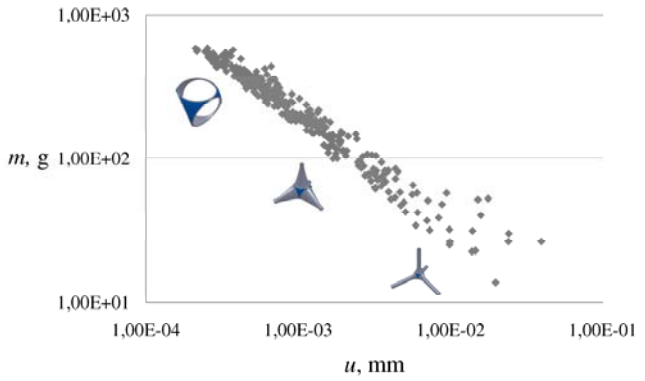

Fig. 7 Distribution of 321 space-filling geometrically consistent design points in the space of total mass m - superelement ray's outer edge displacement u, obtained with constant thickness distribution function

3.3. Topology optimization

The built-in homogenization method based [14] topology optimization module of ANSYS software package was tested for the given loading scheme (Fig. 5). The method is applicable to shells and solids.

Within the task setting of the study, the most appropriate topology optimization criterion from the available was that of minimizing the volume or mass of the superelement. The minimization is subject to a given constraint of maximum increase for the energy of structural static compliance, which was set to 90 percent during the study.

The topology optimization for solids was carried out for the maximum volume available for a single superelement (Fig. 8). The shell optimization option allowed only for 2-dimensional optimization on a given shell surface geometry. Consequently, it could be applied for the definition of thickness variations, including cuts, on surfaces obtained by the optimization of constant thickness geometry models.

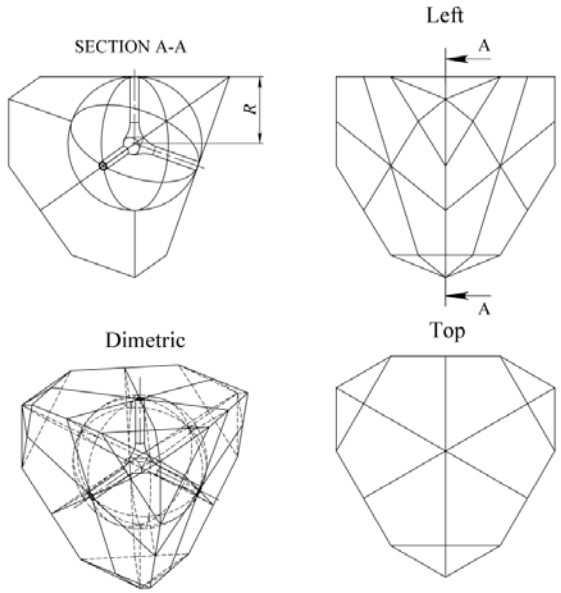

Fig. 8 Design space volume for the superelement's topology optimization showing the position of a topologically equivalent lattice element within

4. Results and discussion

4.1. Preliminary optimization results

Since the constant thickness optimization was intended mainly for general estimation of the optimal geometry, necessary for subsequent shell topology optimization, no detailed analysis of the results was done at this stage. The main conclusion was that the obtained geometry (Fig. 9) approximately matched the shape expected according to the correlation study. Another immediate observation from the numeric results (Table. 2) was that the mass of the obtained structure (27 g) was about an order lower than the upper mass limit, which was an active constraint for the earlier study [6]. This conforms to the general distribution of mass m – ray's edge displacement u (Fig. 7).

Topology optimization for solids yielded geometries having a thick shell structure with protruding struts at the corners (Fig. 10). Specific features of the geometry include the outer and inner shapes of the shell cross-sections, which are approximately hexagonal and circular, respectively. However, the obtained geometry was not directly transferrable to the implemented shell model due to its complexity.

In order to define a thickness distribution function for further study, topology optimization for the shell geometry obtained with constant thickness optimization was carried out. The results (Fig. 11) demonstrated primarily constant thickness distribution with triangular cuts at the centres of spherical surface portions and oblong the cuts along contiguous sides of rays. Locations of the cuts approximately coincide with the regions of lowest stresses for the constant thickness distribution (Fig. 9).

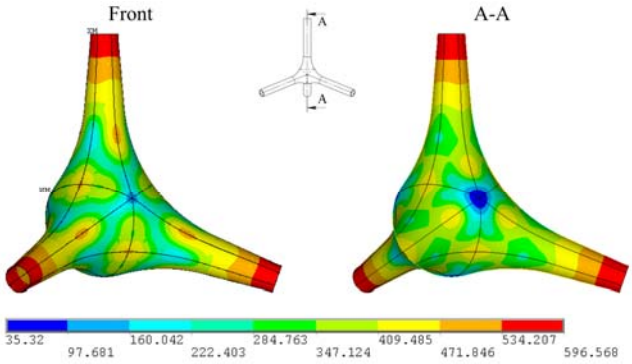

Fig. 9 Equivalent stress distribution (kPa) for superelement's geometry, optimized according to minimum mass criterion, obtained with constant thickness distribution function

Table 2
Values of shape and output parameters corresponding to optimal value of minimum mass criterion, obtained with constant thickness distribution function

Type of parameters	Parameter	Value
Shape parameters	r_1, mm	64.6
	r_2, mm	46.1
	d_2, mm	11.3
	α, deg	10.1
	tk, mm	1.2
	l^a, mm	25.5
	$d_1{}^a$, mm	48.2
Output parameters	U, µJ	20.2
	u, mm	9.68E-03
	m, g	27.1

[a] dependent parameters

4.2. Final optimization results

Based on the results of shell topology optimization, two piecewise defined thickness distribution functions of 6 parameters (see considerations in section 3.2) were defined, having explicit thickness parameters, subject to (4), and relative parameters having ranges of 0…1. The respective meanings of the new parameters are explained in Fig. 12 and Fig. 13. The main difference between the functions is that the first one includes a triangular cut similar to the result obtained by topology optimization, whereas the second one has one more explicit thickness variable compared to the first one.

An additional note regarding the results presented is that in addition to sequential subproblem optimization according to minimum mass criterion small final improvements with upper mass limit, redefined according to the intermediate results obtained, were done according to the aggregate criterion mu, known from the earlier study [6], thereby attaining additional reduction of mass and more uniform stress distributions. According to the earlier

results, the optima obtained with the criterion *mu* could be only local, since it had been found that globally the criterion yields optimal geometries close to maximum stiffness, which correlates positively with the mass *m*.

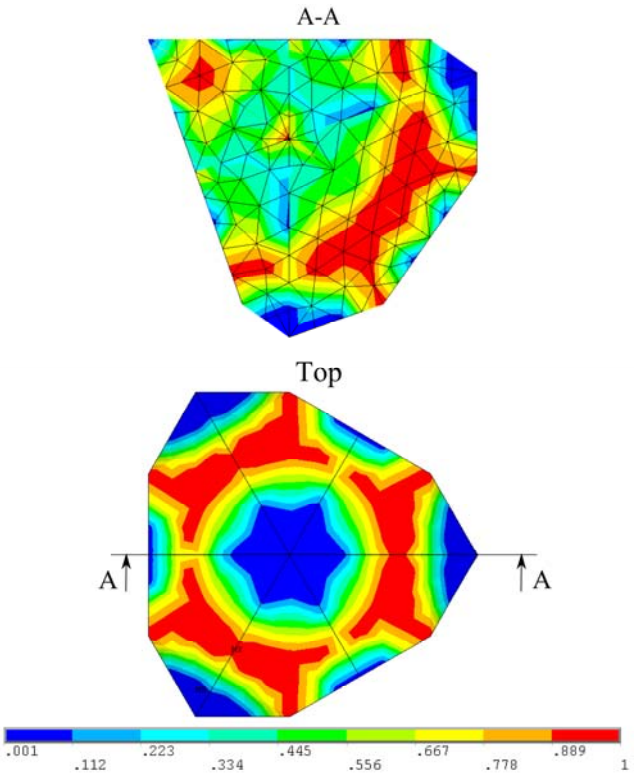

Fig. 10 Pseudodensities of the design volume of the superelement, topologically optimized according to minimum mass criterion

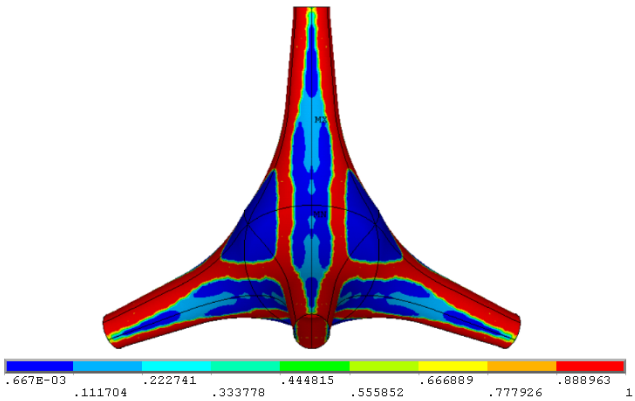

Fig. 11 Pseudodensities of the shell volume of the superelement (right view), topologically optimized according to minimum mass criterion (the shell volume corresponds to minimized mass value, obtained with constant thickness distribution function)

Geometrically both thickness distribution function variants have converged to beam-like shapes (Fig. 14) having small diameters d_1 and d_2 and cone angles α (Table 3). The obtained surface geometries bear topologic and geometric resemblance to open-cell metallic foams with relative density of about 6% [15], which have been modelled by analogous tetrahedral unit cells [16]. The optimized thickness values are similar for both functions. Both geometries have thickening at the location of transition radius r_2 – steep for the first function and gradual for the second – but differ at the location of transition radius r_1 where the first geometry has uniform thickness, which expands up to r_2, whereas the second geometry has a small thickening, which expands onto the spherical surface portion. Generally the geometry corresponding to the first function could be described as slightly inflated compared to the second one.

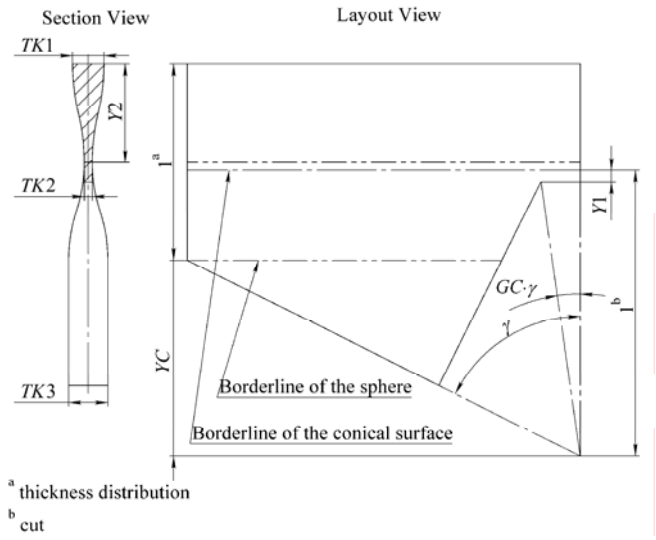

Fig. 12 Normalized piecewise defined thickness distribution for the finite symmetry element of the superelement (Variant 1), where $\gamma = arctan(1/YC)$

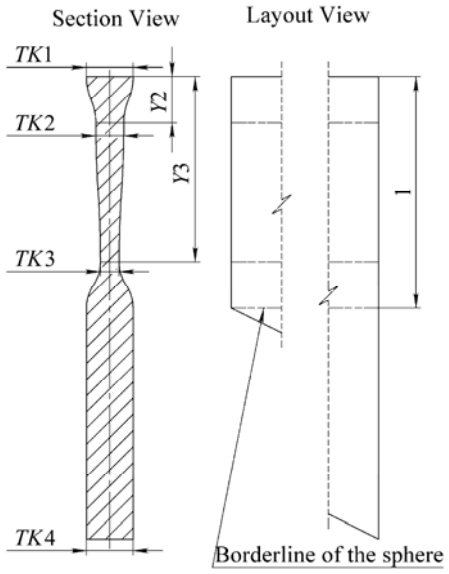

Fig. 13 Normalized piecewise defined thickness distribution for the finite symmetry element of the superelement (Variant 2), where $Y3C = \frac{Y3-Y2}{1-Y2}$

The equivalent stress distribution for the first thickness distribution function (Fig. 15) shows relative uniformity, having distinct low stress concentration regions in the locations corresponding to the oblong cuts yielded by shell topology optimization (Fig. 11) and high stress concentration in the regions of highest curvature. For the second thickness distribution function the equivalent stress (Fig. 16) is distributed rather uniformly as well, having a region of very diverse stress levels on the spherical surface

portion – the location of cut for the first function – and similarly varying stress regions around the circumference at r_1 fillet transition location. Both results allow for the conclusion that some thickness variation, including cut possibility, along a ray's circumference should be defined in order to achieve uniform stress distribution under the given loading. Thus the first thickness distribution function can be considered as better.

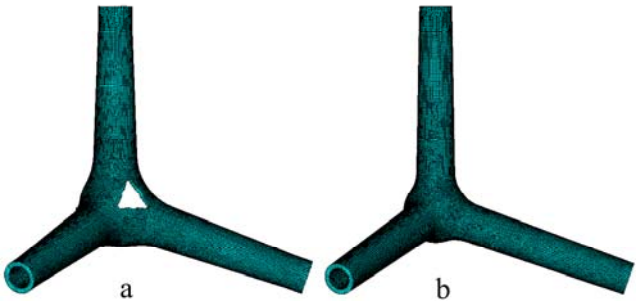

Fig. 14 Superelement's overall geometry (front view), optimized according to minimum mass criterion, obtained with piecewise defined thickness distribution function: Variants 1 (a) and 2 (b)

Table 3

Values of shape and output parameters corresponding to optimal value of minimum mass criterion, obtained with piecewise defined thickness distribution functions

Parameters		Distribution functions	
		Variant 1	Variant 2
Shape parameters	r_1, mm	21.9	14.3
	r_2, mm	17.5	31.2
	d_2, mm	10.4	9.9
	α, deg	4.3	2.5
	$TK1$, mm	1.9	1.9
	$TK2$, mm	1.5	1.4
	$TK3$, mm	1.5	1.7
	$TK4$, mm	-	1.6
	$Y1$	0.57	-
	$Y2$	0.10	0.95
	$Y3C$	-	0.89
	GC	0.10	-
	l^a, mm	54.6	60.1
	$d_1{}^a$, mm	27.6	21.8
Output parameters	U, μJ	20.8	21.0
	u, mm	1.00E-02	1.01E-02
	m, g	23.20	23.27
[a] dependent parameters			

The sensitivity analysis (Table 5) for the present study is purely geometric, since the primary objective function – mass m – is determined by geometry only, the material density being a constant. The analysis shows that for the first thickness distribution function the greatest change in the value of objective function is due to the diameter d_2, which for small α and moderate r_1 and r_2 values is the main determinant of the overall superelement's shape. It is followed by the thicknesses $TK2$ and $TK3$, which define the overall thickness distribution along the axis of a ray. For the second thickness distribution function the sensitivities are similar with the difference that thicknesses $TK1$ and $TK2$ are mainly accountable for the thickness distribution along the axis of a ray.

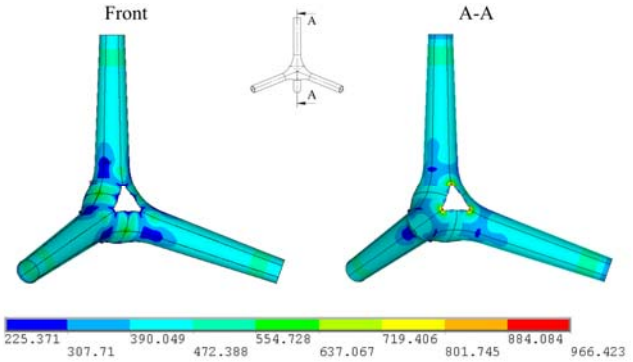

Fig. 15 Equivalent stress distribution (kPa) for superelement's geometry, optimized according to minimum mass criterion, obtained with piecewise defined thickness distribution function (Variant 1)

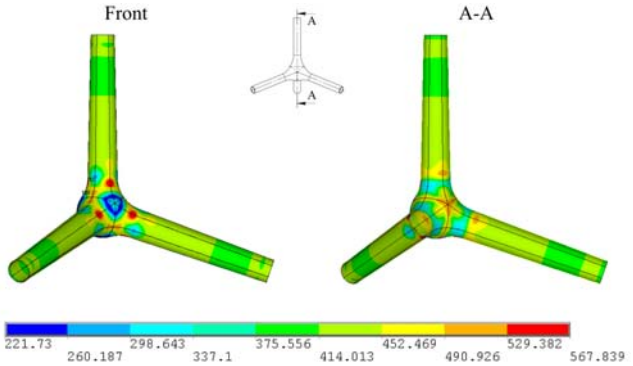

Fig. 16 Equivalent stress distribution (kPa) for superelement's geometry, optimized according to minimum mass criterion, obtained with piecewise defined thickness distribution function (Variant 2)

Additional nonlinear buckling analysis, which included stress stiffening effects, was carried out for both thickness distribution functions (Table 4). Accordingly it could be stated that stability constraints were not relevant for the study. It should be added, however, that for the first function the critical load was about three times lower than for the second one, which is most likely due to the triangular cut, included in the first function.

Table 4

Values of stability loss ratios for superelement geometries, corresponding to optimal values of minimum mass criterion, obtained with piecewise defined thickness distribution functions

Distribution functions	F_{kr}/F
Variant 1	228
Variant 2	658

Based on the obtained types of geometry, for further study from a theoretic point of view the field equations for thick shells of revolution could be directly appli-

cable [17], whereas under certain assumptions regarding boundary conditions a more simple approach for axisymmetric thick truncated conical shells could be considered [18].

Table 5

Change of the minimum mass criterion value due to +1 % change in design variable values with respect to the range of each considered variable, the reference values corresponding to optimized value of the criterion, obtained with piecewise defined thickness distribution functions

Parameters	Mass criterion change	
	Δm^{a}, g	Δm^{b}, g
r_1	-5.98E-03	6.52E-03
r_2	-1.41E-02	9.00E-05
d_2	1.71E-01	1.88E-01
α	3.67E-02	2.55E-02
*TK*1	1.29E-02	1.19E-01
*TK*2	1.08E-01	9.92E-02
*TK*3	1.11E-01	8.89E-03
*TK*4	-	6.08E-03
*Y*1	1.91E-02	-
*Y*2	3.31E-03	8.85E-03
*Y*3*C*	-	-7.58E-04
GC	0.00E+00	-
[a] distribution functions variant 1 [b] distribution functions variant 2		

5. Conclusions

- Close-to-optimum geometries for the superelement of spatial hexagonal lattice have been obtained according to minimum mass criterion under the given conditions.
- The results can be considered as Pareto-optimal [7]: the final choice of parameters is application dependent.
- Possible improvements of the results comprise additional thickness variations, including cuts, along the circumference of superelement's ray.
- Further tasks within the given setting include the implementation of:
  - deadweight of the calculation model;
  - load cases for actual building structure applications;
  - anisotropic nonlinear material definitions;
  - other topologic optimization methods, including level set methods.

Acknowledgements

This work has been supported by the European Social Fund within the project „Support for the implementation of doctoral studies at Riga Technical University".

References

1. **Bervalds, E.** Topological transformations and design of structural systems. -Proceedings of the World Congress on Optimal Design of structural Systems, August 1993, Brazil, Rio de Janeiro, p.153-160.
2. **Christodoulou, L., Venables, J.D.** Multifunctional material systems: The first generation. -JOM Journal of the Minerals, Metals and Materials Soc., 55, 2003, p.39-45.
3. **Haydn, N.G.W.** Multifunctional periodic cellular metals. Phil. Trans. R. Soc. A. 364, 2006, p.31-68.
4. **Lima, C.-H., Jeona, I., Kang, K.-J.** A new type of sandwich panel with periodic cellular metal cores and its mechanical performances. -Materials & Design, 30, 2009, p.3082-3093.
5. **Bervalds, E., Verners, O., Dobelis, M.** The spatial lattice design from a tetrapod-shaped element. -Sci. Proceed. of Riga Tech. Univ.: Constr. Sci., 10, 2009, p. 16-24.
6. **Verners, O., Dobelis, M.** Shape optimization of a superelement of a hexagonal lattice structure. -Sci. Proceed. of Riga Tech. Univ.: Constr. Sci., 11, 2010, in press.
7. **Eschenauer, H., Schnell, W., Olhoff, N.** Applied Structural Mechanics. -Springer, Heidelberg, 1996, -389p.
8. **Bervalds, E., Dobelis, M., Verners, O.** Geometric parameterization of a tetrapod-shaped structural element. -Proceedings of the 10th International Conference on Geometry and Graphics, June 4-5, 2009, Vilnius, Lithuania, p.13-18.
9. **Zienkiewicz, O.C., Scott, F.C.** On the principle of repeatability and its application in analysis of turbine and pump propellers. -Int. J. for Numer. Methods in Eng., 4, 1972, p.445-448.
10. **Bervalds, E., Kaulinsh, J.** Numerical variational method for the synthesis of load bearing building constructions. -Proceedings of the First European Conference on Numerical Methods in Engineering, September, Brussels, Belgium, 1992, p.789-793.
11. **Auzins, J., Janusevskis, A.** Eksperimentu planosana un analize.-Riga Technical University, Riga, 2007. -256p. (in Latvian).
12. Release 11.0 Documentation for ANSYS. Guide to the ANSYS Documentation.
13. **Auzins, J., Janushevskis, A., Rikards, R.** Software tool EDAOpt for optimization of complex systems. -Book of Abstracts: XXXI International Conference Advanced Problems in Mechanics, Russian Academy of Sciences, June 22 - July 2, 2003, Saint Petersburg (Repino), Russia, p.24-25.
14. **Bendsoe, M.P., Kikucki, N.** Generating optimal topologies in structural design using a homogenization method. -Comp. Methods in Appl. Mech. and Eng. 71, 1988, p.197-224.
15. **Nieh, T.G., Higashi, K., Wadsworth, J.** Effect of cell morphology on the compressive properties of open-cell aluminum foams. -Mater. Sci. and Eng., A283, 2000, p.105-110.
16. **San Marchi, C., Mortensen, A.** Deformation of open-cell aluminum foam. -Acta Mater., 49, 2001, p.3959-3969.
17. **Zamani Nejad, M., Rahimi, G.H., Ghannad, M.** Set of field equations for thick shell of revolution made of functionally graded materials in curvilinear coordinate system. -Mechanika. -Kaunas: Technologija, 2009, Nr.3(77), p.18-26.

18. **M. Ghannad, M. Zamani Nejad, G. H. Rahimi**. Elastic solution of axisymmetric thick truncated conical shells based on first-order shear deformation theory. -Mechanika. -Kaunas: Technologija, 2009, Nr.5(79), p.13-20.

O. Verners, M. Dobelis

LENGVASVORIO KETURKOJO SUPERELEMENTO FORMOS OPTIMIZAVIMAS

R e z i u m ė

Tyrimų tikslas – nustatyti iš šešiakampio tipo superelemento (keturkojo) sudaryto optimalios formos tinklelio minimalią masę. Optimizavimas taikant metamodeliavimo metodą, kuris žinomas kaip šalutinės problemos aproksimacija, rėmėsi formos parametrizavimu. Prieš optimizavimą koreliacijos tarp parinktų geometrinių ir struktūrinių parametrų analizei, kurią naudotasi deformacijos parametro riboms ir kūno būsimai geometrijai numatyti, buvo taikomi lotyniško hiperkubo tipo eksperimentiniai planai. Numatomo kevalo storio kitimo funkcijai nustatyti papildomai buvo taikoma topologinė optimizacija. Gauti geometriniai duomenys sutampa su numatytaisiais.

O. Verners, M. Dobelis

SHAPE OPTIMIZATION OF A LIGHTWEIGHT TETRAPOD-LIKE SUPERELEMENT

S u m m a r y

Aim of the study was the determination of minimum mass optimal shape for a hexagon-type (tetrapod-like) lattice superelement. The optimization was shape parameterization based and accomplished by metamodeling approach, also termed subproblem approximation. Prior to it, Latin hypercube type experimental designs were utilized for the study of correlation between selected geometric and structural parameters, which was subsequently used for making predictions as to what limits should be chosen for the constraining deformation parameter and what kind of geometries should be obtained. Additional topology optimization results were used as reference for defining thickness distribution functions for the intended shell geometry. The resulting geometries were in accordance with the expectations.

О. Вернерс, М. Добелис

ОПТИМИЗАЦИЯ ФОРМЫ ОБЛЕГЧЕННОГО ТЕТРАОБРАЗНОГО СУПЕРЭЛЕМЕНТА

Р е з ю м е

Целью настоящего исследования являлось определение минимальной массы оптимальной формы решетки, формированной из суперэлемента гексагонального типа (тетраобразного). Оптимизация базировалась на параметризации формы и была выполнена методом метамоделизации, известным также под названием аппроксимации подпроблемы. Перед этим процессом были использованы экспериментальные планы в виде латинского гиперкуба для исследования корреляции между выбранными геометрическими и структурными параметрами, которая впоследствии была использована для предсказания границ, которые должны быть использованы для ограничения параметра деформации и определения какого вида геометрия должна быть получена. Дополнительно результаты топологической оптимизации были использованы как ссылка для определения функции изменения толщины предполагаемой геометрии оболочки. Полученные геометрии согласуются с предполагаемыми.

Received June 15, 2010
Accepted October 11, 2010